Center for Turbulence Research
Proceedings of the Summer Program 1992

Vortex-induced disturbance field in a compressible shear layer

By D. Papamoschou[1] AND S. K. Lele[2]

The disturbance field induced by a small isolated vortex in a compressible shear layer is studied using direct simulation in a convected frame. The convective Mach number, M_c, is varied from 0.1 to 1.25. The vorticity perturbation is rapidly sheared by the mean velocity gradient. The resulting disturbance pressure field is observed to decrease both in magnitude and extent with increasing M_c, becoming a narrow transverse zone for $M_c > 0.8$. A similar trend is seen for the perturbation velocity magnitude and for the Reynolds shear stress. By varying the vortex size, we verified that the decrease in perturbation levels is due to the mean-flow Mach number and not the Mach number across the vortex. At high M_c, the vortex still communicates with the edges of the shear layer, although communication in the mean-flow direction is strongly inhibited. The growth rate of perturbation kinetic energy declines with M_c primarily due to the reduction in shear stress. For $M_c \geq 0.6$, the pressure dilatation also contributes to the decrease of growth rates. Calculation of the perturbation field induced by a vortex doublet revealed the same trends as in the single-vortex case, illustrating the insensitivity of the Mach-number effect to the specific form of initial conditions.

1. Introduction

It is well known that the Mach number has a powerful effect to suppress the instability and growth of free shear flows. Landau[1] first showed that the vortex sheet becomes stable when the relative Mach number exceeds a critical value ($\sqrt{2}$ for the equal-density case). Early linear analyses (Lin 1953, Gropengiesser 1970, Blumen *et al.* 1975) and single-stream experiments (Sirieix & Solignac 1966) discovered that the growth rates of compressible, finite-thickness shear layers decrease sharply with increasing Mach number. Recent linear analyses (Ragab & Wu 1988, Zhuang *et al.* 1990), computations (Sandham & Reynolds 1989, Lele 1989), and two-stream experiments (Chinzei *et al.* 1986, Papamoschou & Roshko 1988, Samimy & Elliott 1990, Goebel & Dutton 1991) covering a larger range of conditions confirmed the above trends. The experiments, in particular, showed that at high Mach numbers the turbulent shear-layer growth rate decreases to as little as one fifth of the incompressible value. The perturbation levels of velocity decline in a similar fashion (Samimy & Elliott, Goebel & Dutton). Despite these recent gains in the field of

1 University of California, Irvine
2 Stanford University

compressible turbulence, the fundamental physical reason for the stabilizing effect of Mach number remains elusive.

While compressible shear flows typically contain density gradients, density effects alone are not responsible for the large reduction in growth rates. Brown & Roshko (1974) showed that the growth rate of the subsonic, variable-density shear layer changed only by about 50% when the density ratio was varied by a factor of 50. There is, therefore, a large effect associated with the Mach number itself. An exclusive property of Mach number is the ability to cut off communication between parts of the flow, a well-known phenomenon in supersonic flow.

Morkovin (1987) stresses that upstream and cross-flow communication is essential for instabilities at supersonic and hypersonic speeds. His point is primarily based on Mack's (1984) linear stability analysis, where it is shown that the most unstable waves are those whose phase speed is subsonic relative to the free-stream velocity. Morkovin suggests the existence of zones of influence, defined by Mach cones, outside which a disturbance is not felt. The concept of reduced communication at high Mach number has been incorporated into recent turbulence models. Breidenthal's (1990) sonic-eddy model is based on the assumption that turbulent eddies whose rotational Mach number is greater than unity do not participate in fluid entrainment, while those with rotational Mach number of unity or less engulf fluid like incompressible eddies. The mixing-length model of Kim (1991) for a supersonic shear layer assumes that disturbances do not penetrate outside a region bounded by relative sonic velocities.

Morkovin's concept and the models by Breidenthal and by Kim, while conceptually useful, do not explain the fact that stabilization starts at low subsonic values of the Mach number and is practically complete when the velocity difference between the center and the edge of the shear layer becomes sonic (see references above). Furthermore, the fact that the relative velocity is supersonic does not prove that information will not propagate outside the region bounded by the sonic velocity. To address the problem in a more quantitative, although still idealized fashion, Papamoschou (1991) used ray theory to study the acoustic field of a monopole placed inside a shear layer. It was shown that the influence of the monopole diminishes with increasing Mach number but that a low level of communication still exists at supersonic relative speeds. Still, the connection between communication and instability remained a speculative one.

In this study, we explore the link between acoustic field and disturbance motion by direct numerical simulation of a simple instability problem: the impulse response of a shear layer to a localized vorticity perturbation and the change of that response with increasing Mach number. Specifically, we examine the unsteady process by which the shearing of a single vortex, placed in the center of the shear layer, produces velocity, pressure and density fluctuations in the surrounding flow field. Since vortical interactions among eddies are an essential ingredient of turbulence, our simplified problem may serve as a building block for understanding the effect of Mach number on the more complex vortical interactions in realistic shear flows.

2. Initial conditions

The computation is two dimensional, inviscid and temporal, with periodic boundary conditions in the mean-flow direction and non-reflecting boundary conditions in the y-direction. At time $t = 0$, the flow field consists of the shear layer, described by a hyperbolic-tangent velocity profile $U(y)$, with velocity difference ΔU and vorticity thickness $\delta_\omega = 0.1$, and an Oseen vortex (Fig.1).

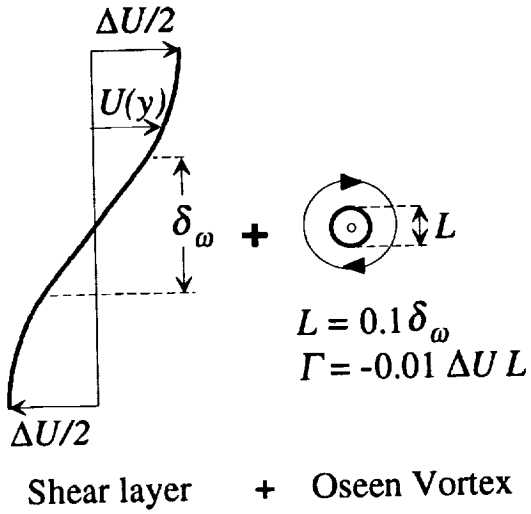

papamos/fig1.ps [1] FIGURE 1. Initial conditions.

The Oseen vortex is a solution to the flow with zero shear and has a tangential velocity

$$v_\theta = \frac{\Gamma}{2\pi r}\left[1 - e^{-\alpha r^2/L^2}\right], \tag{1}$$

where Γ is the circulation, L is the vortex size, and $\alpha = 1.256431$ is chosen such that $v_\theta = v_{\theta,max}$ at $r = L$. The corresponding pressure distribution, derived by the radial momentum equation under the assumption of homentropic flow, is

$$\frac{p}{p_\infty} = \left[1 - \frac{(\gamma-1)\Gamma^2}{4a_\infty^2\pi^2 r^2} f(\alpha r^2/L^2)\right]^{\frac{\gamma}{\gamma-1}} \tag{2}$$

where

$$f(x) = \frac{1}{2} - e^{-x} + \frac{1}{2}e^{-2x} + xEi(-2x) - xEi(-x)$$

with $Ei(x)$ the exponential-integral function and ∞ denoting the unperturbed conditions.

The circulation of the Oseen vortex is fixed here at $\Gamma = 0.01\Delta U L$. Unless otherwise stated, the size of the vortex is $L = 0.1\delta_\omega$. The speed of sound a is constant throughout the flow field. The convective Mach number is

$$M_c = \frac{\Delta U}{2a}$$

with ΔU the velocity difference across the layer. To increase M_c, the velocity difference remains constant and the speed of sound decreases. The M_c range covered here is from 0.1 to 1.25.

For finite shear, the Oseen vortex is no longer a solution to the flow field. As a result, the flow tries to adjust to the new condition by generating an acoustic wave which propagates in all directions and becomes distorted by the mean Mach number gradient. Behind the acoustic wave, a disturbance field is established whose pattern evolves slowly with time. The disturbance velocity field is $\mathbf{u} = (u, v)$ and the pressure perturbation is p.

The computation is advanced in increments of *acoustic time* t whose non dimensional version is $t_a = ta/\delta_\omega$. The corresponding *shearing time* is

$$t_s = tS = t_a \frac{\Delta U}{a} = 2t_a M_c$$

where $S = \Delta U/\delta_\omega$ is the maximum shear. At fixed t_s, a particle at the edge of the shear layer has traveled the same distance, hence the flow has been sheared by the same amount, regardless of the value of M_c. Comparisons among the flow fields at various M_c's will be made at fixed shearing time.

3. Computational Details

The computations were carried out in a domain of size 2 in the mean-flow direction (x) and of size 0.5 in the transverse direction (y). The disturbance vortex was placed at the center of the domain which was discretized by a non-uniform mesh in both directions. In the computations reported in this paper, the mesh contained 200 points in x (with a maximum mesh stretching of 3.2) and 50 points in y (with a maximum mesh stretching of 3.2). Near the vortex the mesh size was 0.0026 in both x and y. Spatial derivatives were evaluated using the sixth-order compact finite differences (Lele 1989, 1992), and third-order compact storage Runge-Kutta scheme was used for time advancement. Periodic boundary conditions in x and "non-reflecting" boundary conditions in y were employed. To make the initial conditions compatible with the periodicity in x, the method of images was used (with two images taken outside each x-boundary). To suppress the spurious generation of 2δ error waves in regions of mesh stretching, compact filtering scheme designed to remove only the near 2δ waves (Lele 1992) was applied to the fields being integrated every 20 time steps. It was verified that the applied filtering produced no significant change in the well-resolved physical disturbances.

4. Results and Discussion

We first present the time evolution of several quantities at $M_c = 0.4$. Fig. 2 shows the vorticity deformation due to the mean velocity gradient. At late times, vorticity is concentrated in a narrow, almost horizontal layer. Even though only the evolution at $M_c = 0.4$ is presented, the vortex shearing seen in Fig. 2 is practically the same for the full range of M_c's covered here. The corresponding evolution in kinematic Reynolds shear stress $-uv$ is depicted in Fig. 3. At $t_s = 0$, the round

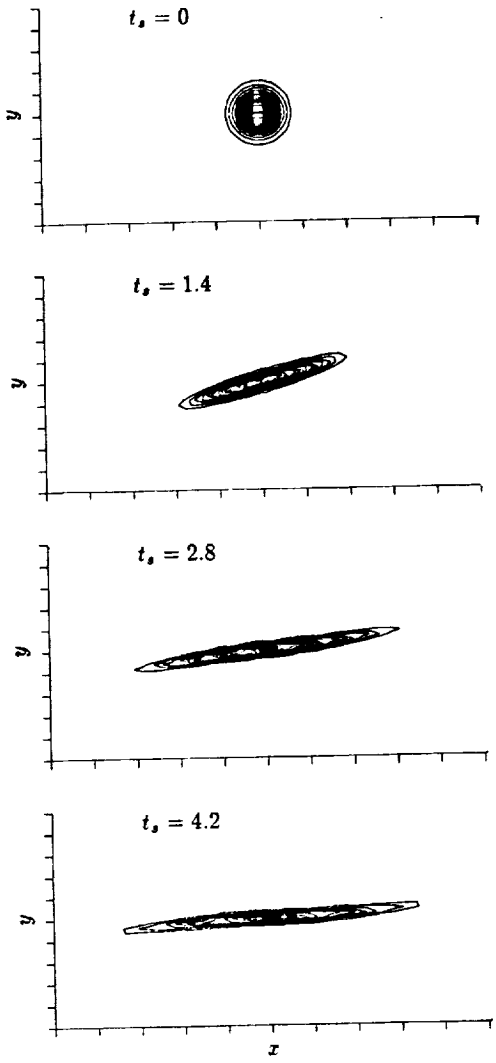

FIGURE 2. Iso-contours of disturbance vorticity $\omega L/\Delta U$ for $M_c = 0.4$. Contour levels: Minimum=-0.075; Maximum=-0.005; Increment=0.005. x-increment=0.02; y-increment=0.01.

vortex has equal amounts of positive and negative shear stress. As time progresses, the negative part vanishes while the positive part occupies a larger part of the flow field. The time development of the divergence is seen in Fig. 4, where the expanding wavefront is evident. As mentioned earlier, the wavefront arises from the reaction of the flow to the initial conditions. Partial reflection of the wave front from the upper and lower boundaries is due to numerical error associated with the boundary conditions.

We now present the Mach number effect on the disturbance field at fixed t_s. Fig.

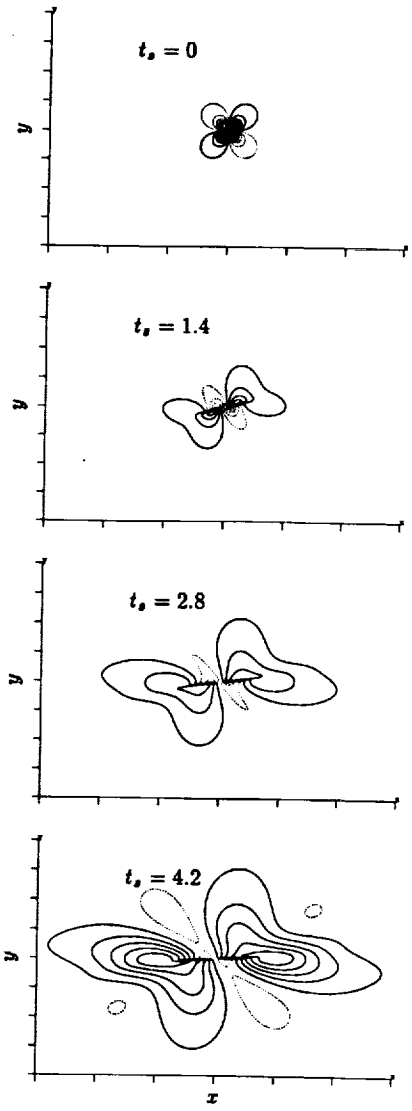

FIGURE 3. Iso-contours of Reynolds shear stress $-uv/(\Delta U)^2$ for $M_c = 0.4$. Contour levels:Maximum=26E-5;Minimum=-26E-5; Increment=3E-5. x-increment=0.1; y-increment=0.05.

5 depicts the magnitude of the pressure perturbation at four different M_c's. The extent and magnitude of the field decrease rapidly with increasing Mach number. At $M_c = 1.25$, the pressure field is reduced to a narrow transverse zone. The same trend is seen for the disturbance-velocity magnitude, shown in Fig. 6, and for the shear stress, shown in Fig. 7. Comparison of Figs. 5 and 7 shows that the decline

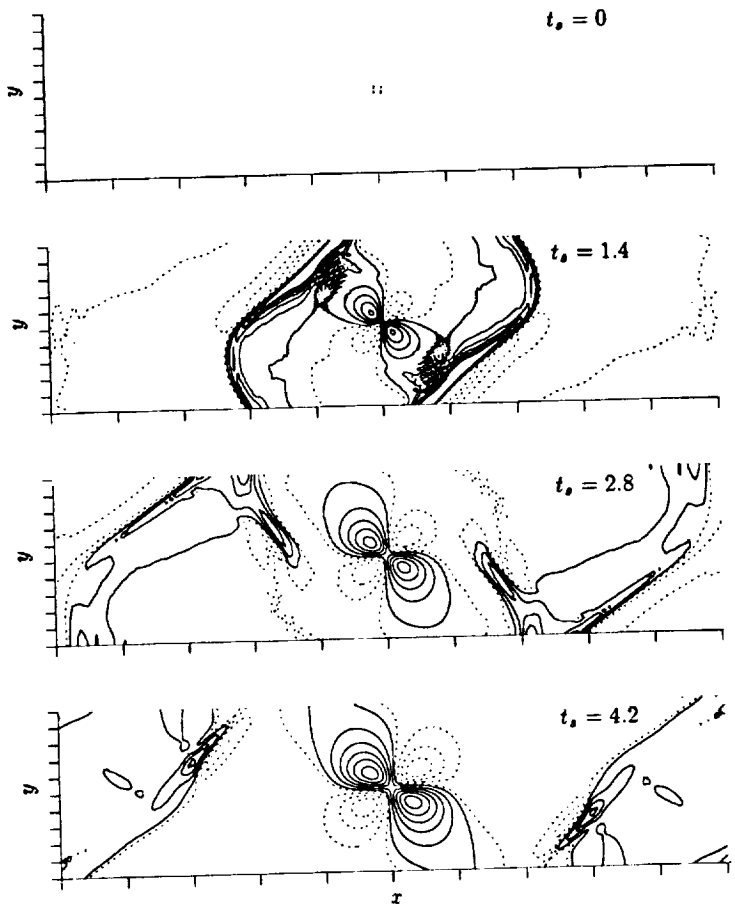

FIGURE 4. Iso-contours of divergence $\nabla \cdot \mathbf{u}\ L/\Delta U$ for $M_c = 0.4$. Contour levels: Maximum=0.025; Minimum=-0.017; Increment=0.004. x-increment=0.2; y-increment=0.05.

in magnitude and extent of the p and $-uv$ fields is very similar.

The pressure pattern seen in Fig. 5 reveals some very noteworthy effects of compressibility on the vortex influence. Evidently, at high M_c, the influence of the vortex does not propagate in x but stays confined within a narrow, transverse region. Interestingly, the vortex still communicates to edges of the shear layer, even when the relative velocity is supersonic. This implies that the turbulence models mentioned in the Introduction, which assume that all interactions occur within the a layer bounded by sonic velocities (Breidenthal 1990, Kim 1991), are overly idealized. The lack of communication in the x-direction may explain the lack of vortex pairing and shear-layer roll up at high M_c.

We now examine the source term for the transverse component of the kinetic energy $\frac{1}{2}v^2$, namely $-v\partial p/\partial y$. Note that generation of $\frac{1}{2}v^2$ does not involve the mean shear, thus is directly related to the pressure field. Fig 8 shows the source

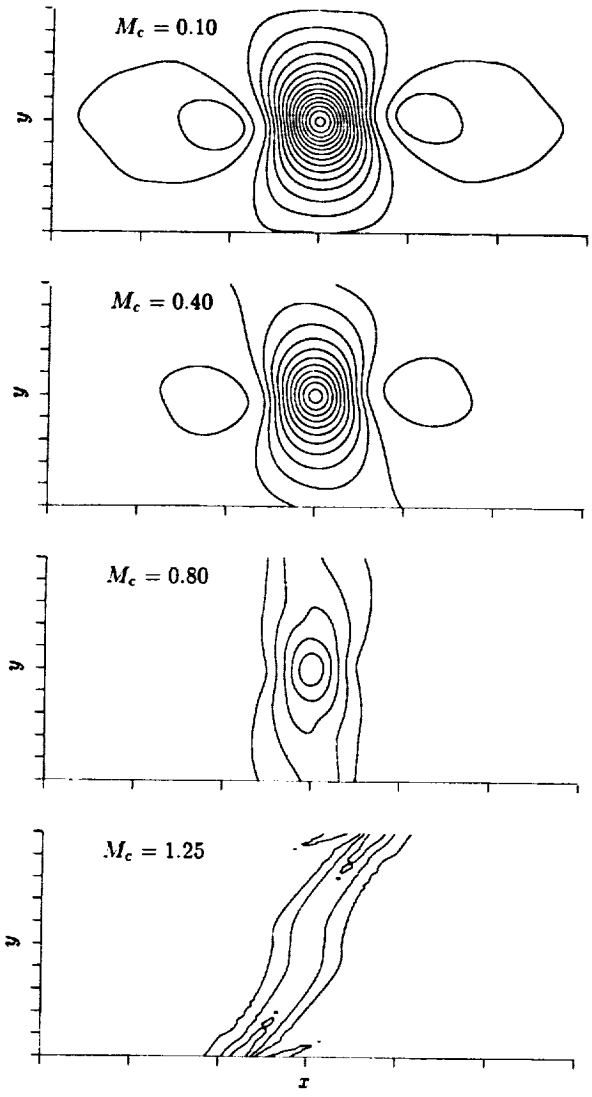

FIGURE 5. Iso-contours of pressure disturbance magnitude $|p|/(\rho_\infty \Delta_U^2)$ at $t_s = 4.2$. Contour levels: Maximum=0.032; Minimum=0.002; Increment=0.002. x-increment=0.2; y-increment=0.05.

term dramatically decreasing with increasing M_c, practically vanishing at $M_c = 0.8$. At $M_c = 1.25$, the radiative nature of the flow, coupled with boundary-condition errors, make this term reappear in roughly-equal negative and positive amounts, so its integrated contribution is near-zero. The decline of $-v\partial p/\partial y$, and the resulting reduction in $|v|$, are the direct result of the reorientation of the pressure field due to the Mach number. Since $|u|$ and $|v|$ are of the same order, the shear stress $-uv$ is also reduced, as seen in Fig. 7. The lower $-uv$, in turn, causes a decrease in the growth rate of the overall fluctuation kinetic energy, which will be shown later.

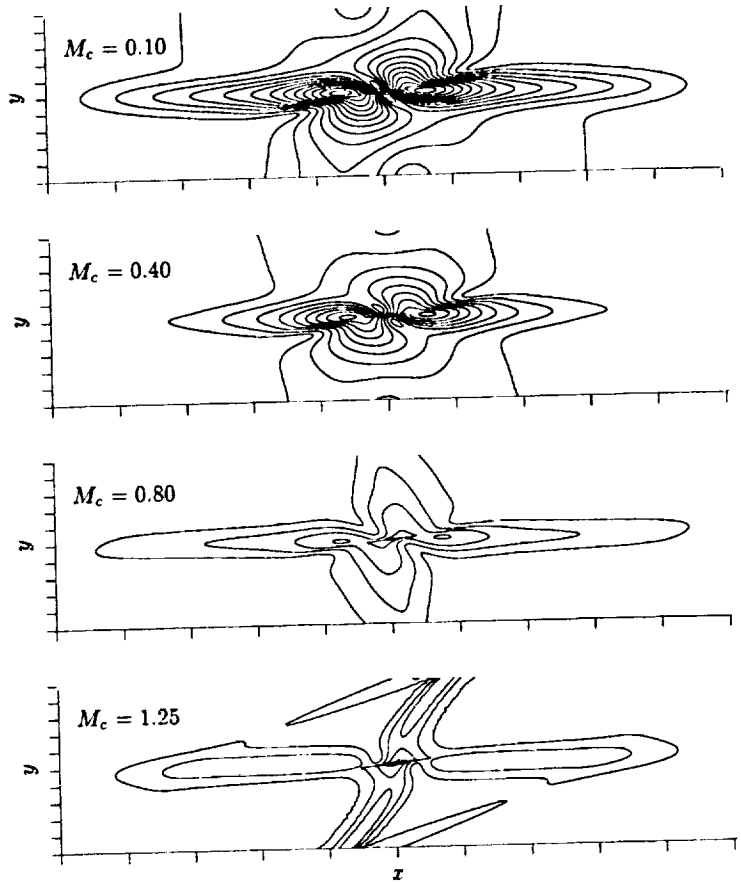

FIGURE 6. Iso-contours of disturbance velocity magnitude $|\mathbf{u}|/\Delta U$ at $t_s = 4.2$. Contour levels: Maximum=0.028; Minimum=0.002; Increment=0.002. x-increment=0.2; y-increment=0.05.

The same mechanism has been observed to reduce the kinetic-energy growth rate in compressible homogeneous sheared turbulence (Blaisdell *et al.* 1991).

To verify that the observed trends are due to the mean-flow Mach number and not due to the Mach number $M_L = M_c L/\delta_\omega$ across the vortex, we varied M_L by changing the vortex size, keeping the circulation fixed, and compared the resulting disturbance fields. Fig. 9 offers two such comparisons: at $M_c = 0.4$, M_L changed from 0.04 to 0.08, while at $M_c = 0.8$, M_L changed from 0.08 to 0.04. If M_L were the critical parameter, one would expect similarity between the fields at $M_L = 0.04$ and between the fields at $M_L = 0.08$. This is clearly not the case, and, even though details near the vortex core change with size, the overall extent and magnitude of the fields depend only on M_c.

A quantity of great interest in any instability problem is the fluctuation kinetic energy $k = \frac{1}{2}\mathbf{u}\cdot\mathbf{u}$ and its generation terms. For our inviscid, two-dimensional flow,

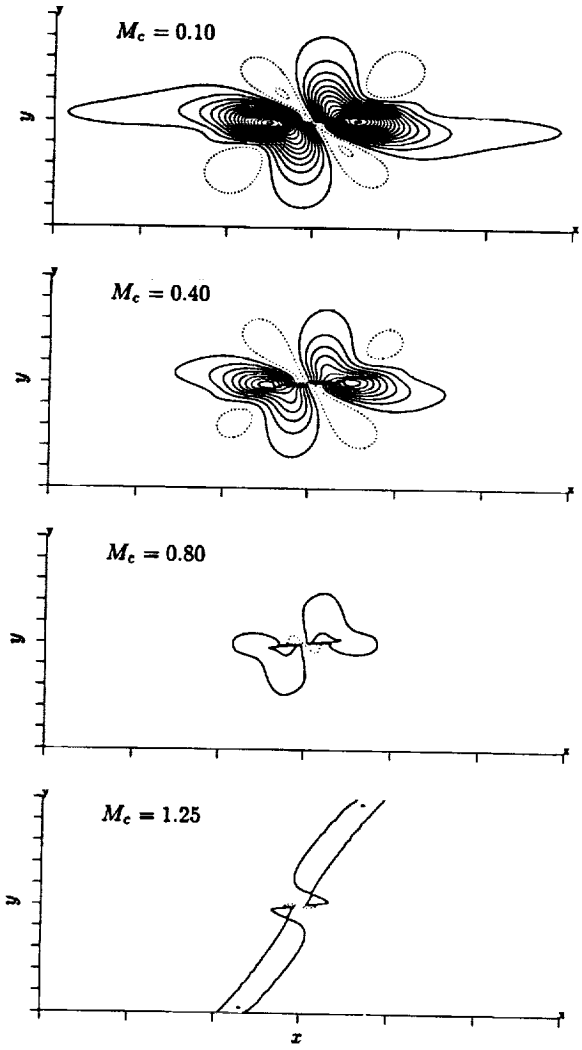

FIGURE 7. Iso-contours of Reynolds shear stress $-uv/(\Delta U)^2$ at $t_s = 4.2$. Contour levels: Maximum=33E-5; Minimum=-5E-5; Increment=2E-5. Negative values are denoted by dotted lines. x-increment=0.2; y-increment=0.05.

the instantaneous k is described by

$$\frac{\partial k}{\partial t} + U\frac{\partial k}{\partial x} = -uv\frac{dU}{dy} + p\nabla\cdot\mathbf{u} - \nabla\cdot(p\mathbf{u}) - \nabla\cdot(k\mathbf{u}) \tag{3}$$

The terms on the right-hand side are called production due to shear stress, pressure dilatation, pressure transport, and kinetic-energy transport. We examine the time evolution of the quantities in Eq. 3, integrated in space over our computational domain.

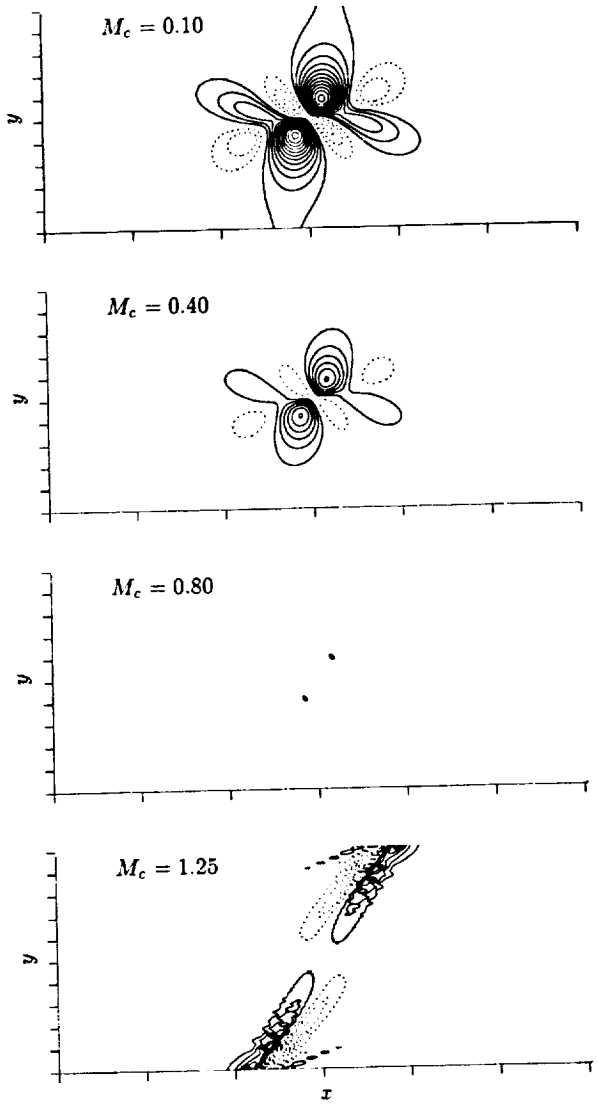

FIGURE 8. Iso-contours of $(v\partial p/\partial y)/\rho_\infty \Delta U^3$ at $t_s = 4.2$. Contour levels: Maximum=0.0026; Minimum=-0.0022; Increment=0.0002. Negative values are denoted by dotted lines. x-increment=0.2; y-increment=0.05.

The growth of the disturbance kinetic energy versus time for different M_c's is seen in Fig. 10(a). As expected, the higher M_c's produce significantly lower growth rates. At early times, the growth rate of the $M_c = 1.25$ case slightly exceeds that of the $M_c = 0.8$ case. This is probably due to the longer presence of the wavefront in the computational domain at $M_c = 1.25$. Recall that M_c is increased by lowering the speed of sound, thus the wavefront and its velocity perturbation take longer time to propagate outwards at high M_c. By late times, however, the $M_c = 1.25$ growth rate is seen to saturate and decline below the $M_c = 0.8$ curve. Figure 10(b) shows

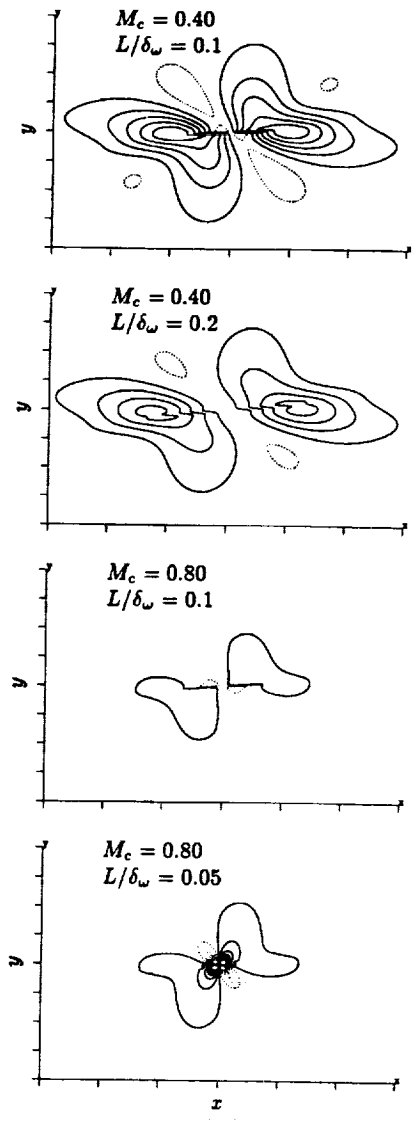

FIGURE 9. Iso-contours of Reynolds shear stress $-uv/(\Delta U)^2$ at $t_s = 4.2$ for variable initial vortex size L. Contour levels: Maximum=26E-5; Minimum=-26E-5; Increment=3E-5. Negative values are denoted by dotted lines. x-increment=0.1; y-increment=0.05.

the production due to shear stress, which also declines rapidly with increasing M_c. The pressure dilatation term, seen in Fig 10(c), is much lower than the production term for $M_c = 0.1$ and 0.4, but becomes comparable at the higher M_c's. Thus, the decline in growth rates, most of which occurs at subsonic M_c, is primarily due to

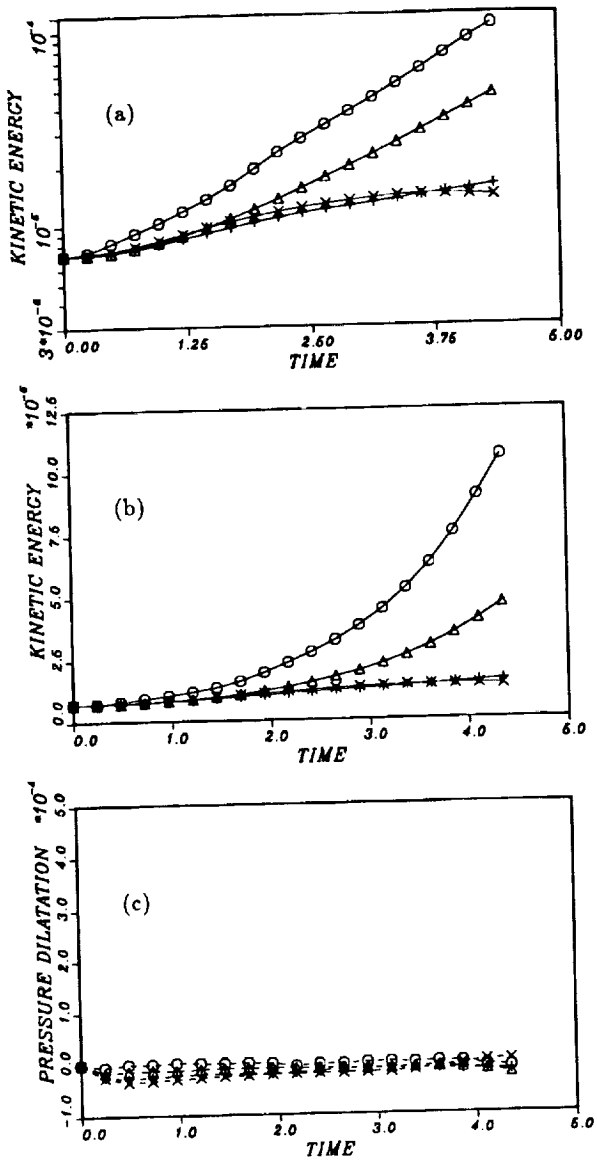

FIGURE 10. Evolution of spatially-integrated quantities versus t_s for variable M_c: (a) perturbation kinetic energy; (b) production due to shear stress; (c) pressure dilatation. o $M_c = 0.1$; $\triangle$ $M_c = 0.4$; + $M_c = 0.8$; $\times$ $M_c = 1.25$.

the reduction in shear stress. The pressure dilatation term becomes significant at high-subsonic and supersonic M_c and makes the overall generation of kinetic energy even smaller. The pressure transport and kinetic-energy transport terms were found to be negligible compared to the previous two terms.

To test the sensitivity of the Mach-number effect on initial conditions, we replaced

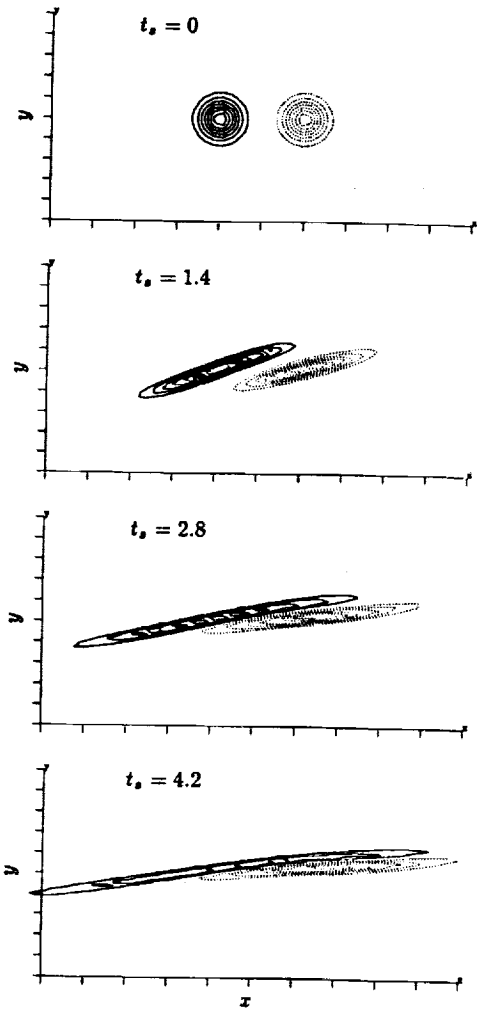

FIGURE 11. Iso-contours of dipole disturbance vorticity $\omega L/\Delta U$ for $M_c = 0.4$. Contour levels: Minimum=-0.07; Maximum=0.07; Increment=0.01. Negative values are denoted by dotted lines. x-increment=0.02; y-increment=0.01.

the single vortex by a vortex dipole. The dipole vortices have the same circulation and size as the previous single vortex, and are separated by a distance $4L$. The shearing of the dipole versus t_s is shown in Fig. 11. At late times, the positive vorticity is stretched a little more than the negative one, probably because of the interaction between the two vorticity regions. The Reynolds shear stress versus M_c is depicted in Fig. 12, where its magnitude and extent are seen to shrink rapidly with increasing M_c, as in the single-vortex case. Additionally, we reversed the circulation of the single vortex, producing a counter-clockwise motion. The magnitude and extent of perturbation fields remained identical to those of the clockwise vortex.

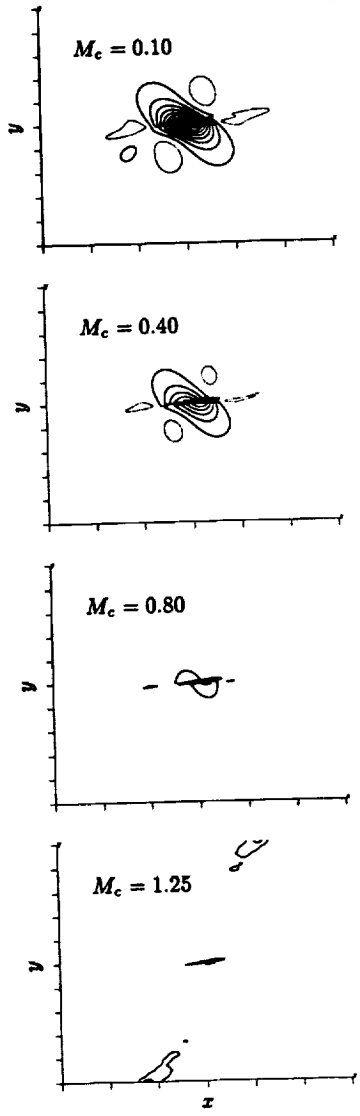

FIGURE 12. Iso-contours of dipole Reynolds shear stress $-uv/(\Delta U)^2$ at $t_s = 4.2$. Contour levels: Maximum=21E-5; Minimum=-5E-5; Increment=2E-5. Negative values are denoted by dotted lines. x-increment=0.1;y-increment=0.05.

Evidently, the precise form of the initial condition does not affect the stabilizing influence of the mean-flow Mach number.

To illustrate the robustness of the high-M_c features observed here, we make qualitative comparisons among pressure fields at $M_c = 1.25$ generated by three different

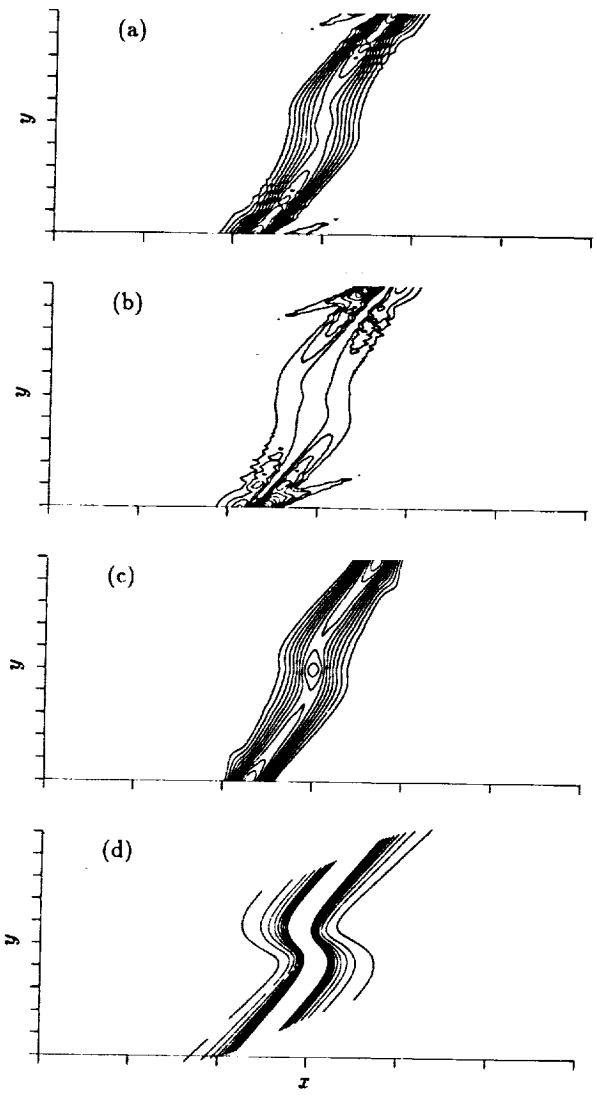

FIGURE 13. Qualitative comparison of $M_c = 1.25$ pressure disturbance fields. Direct simulation:(a) vortex monopole; (b) vortex dipole; (c) acoustic monopole. Geometric acoustics theory:(d) acoustic monopole. x-increment=0.2; y-increment=0.05.

initial conditions. In Fig. 13, the pressure-disturbance fields for (a) a single vortex, (b) a vortex dipole, and (c) an acoustic monopole are displayed. The acoustic monopole has an initial-pressure field same as in the single Oseen vortex, but the vorticity is now zero. All three features look very similar, which once again shows their dominance by the mean-flow Mach number and their independence from details of the initial condition. Fig. 13(d) depicts the field of an acoustic monopole, computed by the simple energy-invariance method of geometric acoustics (for details

see Ref. 19). Even though geometric-acoustics theory is only applicable to high-frequency sources, the calculated pressure field resembles very much those computed by direct numerical simulation.

5. Conclusions

The disturbance field generated by the shearing of a vortex placed in the center of a compressible shear layer has been studied by means of direct numerical simulation. The magnitude and extent of the induced pressure and velocity fields diminish rapidly with increasing convective Mach number M_c, with most of the decrease occurring at subsonic values of M_c. At $M_c > 0.8$, the influence of the vortex is reduced to a zone of narrow streamwise extent. The vortex still communicates to the edges of the shear layer, although communication in the mean-flow direction is practically cut off. Perturbation kinetic-energy growth rates decrease with increasing M_c, primarily due to reduction of the Reynolds shear stress. Pressure dilatation contributes to the decline in growth rates for $M_c > 0.6$. The trends observed here are insensitive to the specific form of the initial disturbance and are a result of the mean-flow Mach number.

REFERENCES

BREIDENTHAL, R. 1990 The sonic eddy–A model for compressible turbulence. *AIAA-90-0495.*

BLAISDELL, G. A., MANSOUR, N. N. & REYNOLDS, W. C. 1991 Numerical simulations of compressible homogeneous turbulence, Report No. TF-50, Dept. of Mech. Engrg., Stanford University.

BLUMEN, W., DRAZIN, P. G., & BILLINGS, D. F. 1975 Shear layer instability of an inviscid compressible fluid. Part 2. *J. Fluid Mech.* **71,** 305-316.

BROWN, G. L. & ROSHKO, A. 1974 On density effects and large-scale structures in turbulent mixing layers. *J. Fluid Mech.* **64,** 775-781.

CHINZEI, N., MASUYA, G., KOMURO, G., MURAKAMI, T. & KUDOU, K. 1986 Spreading of two-stream supersonic mixing layers. *Phys. Fluids.* **29,** 1345-1347.

GOEBEL, S. G. & DUTTON, J. C. 1991 Experimental study of compressible turbulent mixing layers. *AIAA J.* **29,** 538-546.

GROPENGIESSER, H. 1970 Study of the stability of boundary layers in compressible fluids *NASA TT-F-12,* 786.

KIM, S. C. 1990 New mixing length model for supersonic shear layers. . *AIAA J.* **28,** 1999-2000.

LANDAU, L. 1944 Stability of tangential discontinuities in compressible fluid. *Dokl. Akad. Nauk. SSSR.* **44,** 139-141.

LELE, S. K. 1989 Direct numerical simulation of compressible shear flows. *AIAA-89-0374.*

LELE, S. K. 1992 Compact finite difference schemes with spectral-like resolution, to appear in *Computational Physics.*

LIN, C. C. 1953 On the stability of the laminar region between two parallel streams in a gas. *NACA Report TN 2887.*

MACK, L. M. 1984 Boundary-layer linear stability theory. *AGARD Report R-709.*

MORKOVIN, M. V. 1987 Transition at hypersonic speeds. *NASA-CR-178315, ICASE Interim Report 1.*

PAPAMOSCHOU, D. & ROSHKO, A. 1988 The turbulent compressible shear layer: an experimental study. *J. Fluid Mech.* **197,** 453-477.

PAPAMOSCHOU, D. 1991 Effect of Mach number on communication between regions of a shear layer. *Eighth Symp. Turb. Shear Flows.*

RAGAB, S. A. & WU, J. L. 1988 Instabilities in turbulent free shear layers formed by two supersonic streams. *AIAA-88-0038.*

SAMIMY, M. & ELLIOTT, G. S. 1990 Effects of compressibility on the characteristics of free shear layers. *AIAA J.* **28,** 439-445.

SANDHAM, N. & REYNOLDS, W. 1990 The compressible mixing layer: linear theory and direct simulation. *AIAA J.* **28,** 618-624.

SIRIEIX, M. & SOLIGNAC, J. L. 1966 Contribution a l'etude experimentale de la couche de melange turbulent isobare d'un ecoulement supersonique. *Symposium on Separated Flow, AGARD Conf. Proc.* **4,** 241-270.

ZHUANG, M., KUBOTA, T. & DIMOTAKIS. P. E. 1990 Instability of inviscid, compressible shear layers. *AIAA J.* **28,** 1728-1733.